A NEW EXPERIMENTAL TECHNIQUE FOR THE MEASUREMENT OF THE WIND-INDUCED MOTION OF A CROP CANOPY

Charlotte Py, Emmanuel de Langre, Pascal Hémon
Department of Mechanics, LadHyX, CNRS-Ecole Polytechnique, 91128 Palaiseau, France

Bruno Moulia
UEPF-INRA, 86600 Lusignan, France

Olivier Doaré
ENSTA, 91761 Palaiseau, France

ABSTRACT

We present here a simple spatio-temporal technique based on image correlation to measure the wind-induced motions of crop canopies. The tests were lead on wheat and alfalfa fields under wind. The motion is video-recorded from the side of the field. In a first step we take advantage of the natural periodicity of a crop to correct the distorsion due to perspective. In a second step we use the natural crop heterogeneity to identify motions between successive images. The computation is based on Particle Image Velocimetry (PIV) algorithms. The Bi-Orthogonal Decomposition of the velocity field then reveals large coherent structures that scale with typical wavelength of wind fluctuation over canopies.

1. INTRODUCTION

The study of wind-induced plant motions has been motivated by lodging problems in crops and their economical consequences (Farquhar et al, 2000). Recently, biomechanical studies on thigmomorphogenesis (Coutand et al, 2000), the effect of wind on plants growth, has brought new interest in this field of research.

The fluctuation of wind over canopies has been widely studied (see Finnigan (2000) for a review). Wind velocity measurement on various canopies have revealed the existence of large coherent structures propagating over the canopy surface and responsible for a large part of the transfer of momentum to the crop. Those structures are created by an instability mechanism similar to that of a mixing layer (Raupach et al, 1996).

Despite large sets of measurements on wind velocities, no direct measurements of global plants motion in a canopy with wind have been done. Contact sensors are limited to the measure of a few individual plants motions (Flesch and Grant, 1992). Moreover the compliance and lightness of crop plants make difficult the use of sensors without disturbing the motion. It thus appears necessary to developp a non-contact technique with high spatial resolution.

We propose here a simple optical measurement technique that provides the spatio-temporal velocity field of the surface of crop canopies.

The experiments took place at INRA Lusignan (France) in external conditions. We filmed the motions of two wheat and alfalfa crop fields under natural wind of about 4 m/s mean velocity (Figure 1). The movies were recorded from the side of the field with a digital video camera mounted on a 2.5 meter high tripod at 25 images per second. We took several dozens of 10 second sequences on both wheat and alfalfa motions, of which a few typical results are presented here. Each movie is transformed in a sequence of images. We first correct the perspective distorsion of the images. Then we compute the local displacements between consecutive images using a Particle Image Velocimetry technique. In order to extract the main features of the motion, we apply a Bi-Orthogonal Decomposition to the resulting velocity field. This enables to show the existence of large scale coherent structures and propagation properties of the plants motion.

We first detail the three steps of the technique, i.e. image distorsion rectification , velocity measurements, and Bi-Orthogonal Decomposition in sections 2, 3 and 4 respectively. Then we show a typical exemple on alfala crop motion and discuss a few results in section 5.

Figure 1: *Alfalfa field under wind.*

2. IMAGE DISTORSION RECTIFICATION

As the movies are recorded from the side of the crop field, the images are distorted by perspective. We correct the distorsion before exploiting the images for velocity measurements.

A regular grid seen slantwise would be distorted by perspective as shown Figure 2a. On the distorted image both the horizontal and vertical mesh sizes decrease from the bottom to the top of the image. Measuring their evolutions and ratio allows to determine the parameters governing the perspective geometrical transformation Φ: the shot angle Θ and the distance from the camera to the center of the grid d. Then by applying the inverse transformation Φ^{-1} to the distorded image, the straight image as seen from a top view is rebuild (Figure 2b).

A classical method to correct our images would be to plant regularly spaced targets in the field and use their position on the image as indicators of the perspective distorsion, as for a grid. But it is difficult to plant many targets in a grown field without spoiling the crop.

We thus measure the distorsion by exploiting the natural regularity of a crop as reference. Seen from above and from far enough a crop field surface is homogeneous and isotropic. We can use its natural regularity as a reference mesh. We define a wavelength characteristic of the crop image, which plays the role of the mesh size. This wavelength λ typically scales with the distance between two plants. On perspective images the horizontal and vertical wavelengths, λ_x and λ_y, vary from the bottom to the top of the image. Measuring their evolutions allows to estimate Θ and d, as for a grid.

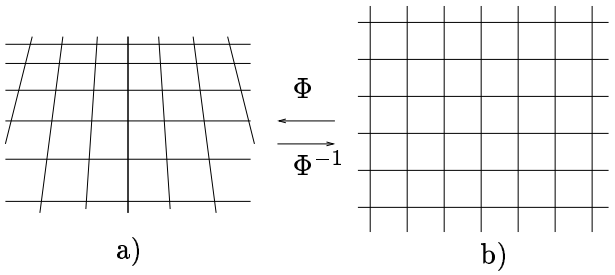

Figure 2: *a) Slantwise view of a regular grid. b) Top view of the same grid.* Φ *is the perspective geometrical transformation and* Φ^{-1} *the correction to apply.*

The characteristic wavelength is computed statistically from the grey value signal of the image. The wavelength λ_i along the direction i is approximated as

$$\lambda_i = 2\pi \frac{< g >}{< \frac{\partial g}{\partial x_i} >}, \qquad (1)$$

where g is the local level of the grey signal and $< \cdot >$ is the standard deviation. Each image of a sequence is then corrected by applying the inverse geometrical transformation Φ^{-1} (see Figure 3 for an exemple on an alfalfa field). The grey signal on the new pixel mesh is then interpolated from the original pixel mesh. The domain is finally restricted to a rectangular geometry.

The rectification process leads to a sequence of straight images with homogeneous lengths scales.

3. VELOCITY MEASUREMENTS USING A PIV TECHNIQUE

The velocity measurement technique is based on standard Particle Image Velocimetry (PIV) (Raffel et al, 1998) but it is applied to the calculation of the crop surface motion, instead of the fluid dynamics. Here the crop canopy itself plays the role of particle tracers : the small scale heterogeneities of the canopy (ie: leaves, spikes...) allow to detect local displacements of the crop surface. Using such natural tracers provides the advantage of a high spatial resolution. Also, as opposed to standard PIV, no artificial light is needed: standard sun light is sufficient to detect the plants motion.

Each image of a sequence is thus divided into small overlapping subwindows. The optimal size of a subwindow scales with the small patterns of the crop image, such as a group of a few leaves. We compute the local displacement of a subwindow between two consecutive images at 0.04 s

time interval. To do so, we seek locally for the peak of the cross correlation function between two small regions from consecutive images. The position of the peak relative to the center of the first subwindow gives the local displacement between time t and $t + \Delta t$. Computations are performed using classical PIV algorithms including correction routines (signal to noise ratio, local and global filters, double pass calculation...).

For each sequence the velocity measurement process leads to the spatio-temporal velocity field $\mathbf{U}(\mathbf{x}, \mathbf{y}, \mathbf{t})$ of the crop surface. Figure 4 is a typical exemple of instantaneous velocity field obtained from a movie of alfalfa crop under wind.

4. POST-PROCESSING USING B.O.D.

In order to extract the main features of the plants motions, we use a Bi-Orthogonal Decomposition (BOD) of the velocity field (see Hémon and Santi (2003) for a review on BOD). It yields the following decomposition of the velocity field

$$\mathbf{U}(\mathbf{x}, \mathbf{y}, \mathbf{t}) = \sum_{\mathbf{k=1}}^{\mathbf{N}} \alpha_{\mathbf{k}}\, \mu_{\mathbf{k}}(\mathbf{t})\, \mathbf{\Psi_k}(\mathbf{x}, \mathbf{y}). \quad (2)$$

The spatial modes $\mathbf{\Psi_k}(\mathbf{x}, \mathbf{y})$, or *topos*, associated to the set of eigenvalues α_k^2 are the eigenmodes of the spatial correlation operator. Simultaneously the temporal modes $\mu_k(t)$, or *chronos*, associated to the same set of eigenvalues, are the eigenmodes of the temporal correlation operator. In this case, the *chronos* are first computed and the *topos* are deduced from inversion of the decomposition equation (2).

Note that here the signal to analyse is two-dimensionnal in space. The correlation calculation thus takes into account the bidimensionality of the problem (correlations between the x and y components of $\mathbf{U}$).

In the decomposition (2), the spatio-temporal modes $(\mu_k, \mathbf{\Psi_k})$ are ranked by decreasing order of their contribution in the total kinetic energy: the eigenvalue α_k^2 represents the kinetic energy of the k^{th} spatio-temporal mode. The rate of convergence of the decomposition is a test of the presence of large coherent structures. With a good convergence rate the first sets of *chronos* and *topos* are the most representative of the motion characteristics. Figures 6, 7 and 8 show exemples of two most energetic *topos* and corresponding *chronos*.

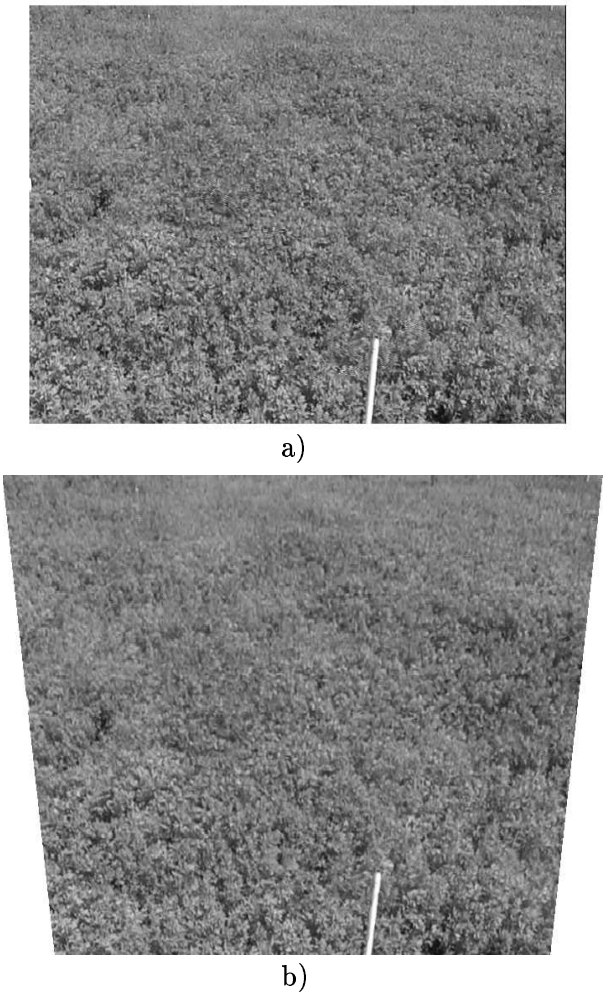

Figure 3: *Initial image (a) of the alfalfa crop and corrected image (b) .*

Figure 4: *Instantaneous velocity field between t and $t + \Delta t$ of the alfalfa crop. Scale of velocities: maximum velocity is here 2.9 m/s.*

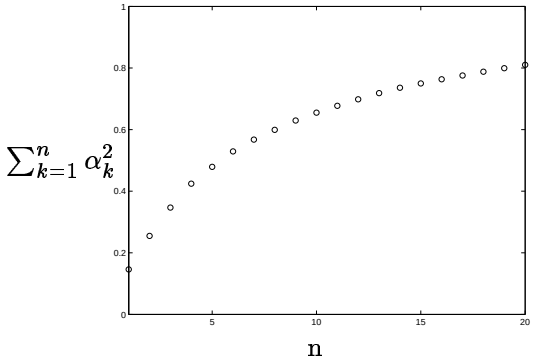

Figure 5: *Fraction of the total kinetic energy recovered from the decomposition as a function of the number of spatio-temporal modes considered.*

5. APPLICATION AND DISCUSSION

We present here an illustration of the technique on a 10 seconds movie of alfalfa crop motion. Figure 3 illustrates the rectification process. We used here the following rectification parameters: $\Theta = 29°$ and $d = 1236$ pixels. The wavelength λ_i derived from equation (1) is about 10 pixels. In this particular crop, the order of magnitude of the distance between plants is about 4 cm. This leads to approximately $d = 5$ m.

Figure 4 shows the velocity field of the alfalfa crop surface at a given time computed with PIV algorithms. We checked the qualitative accuracy of the computed motions with respect to the movie. Quantitative aspects of the PIV process were tested on controlled motions in laboratory.

In the upper fourth of the images the computed velocities are here always smaller. This may be due to a bias in the perspective correction procedure or a poor accuracy of the PIV technique resulting from the small amplitudes of motion in the original image.

Figure 5 shows the convergence of the Bi-Orthogonal Decomposition. When considering only fifteen *chronos-topos* couples of the decomposition, more than 75 % of the total kinetic energy is recovered. This leads to a susbstantial reduction of the number of degrees of freedom of the system: from 5.10^5 (2000 in space times 250 in time) to 3.10^4 (15 times 2000 in space plus 250 in time). This shows a good convergence of the BO decomposition and indicates the strong coherence of the crop surface motion.

Figures 6, 7 and 8 represent the two most energetic spatio-temporal modes (*topos* and corresponding *chronos*). The *topos* (Figures 6 and 7) reveal large scale organized motions such as sweeps and vortices. The vorticity fields of the *topos* (Figure 9 and 10) offer a good visualisation of the coherent stuctures. They appear as large parallel strips. The corresponding wavelength Λ is about 1 m, comparable with that observed by Finnigan (2000) in the structures of wind over canopies. The divergence fields of the *topos*, Figure 11 and 12, also show patterns but less emphazised and without the directionnal anysotropy of the vorticity field.

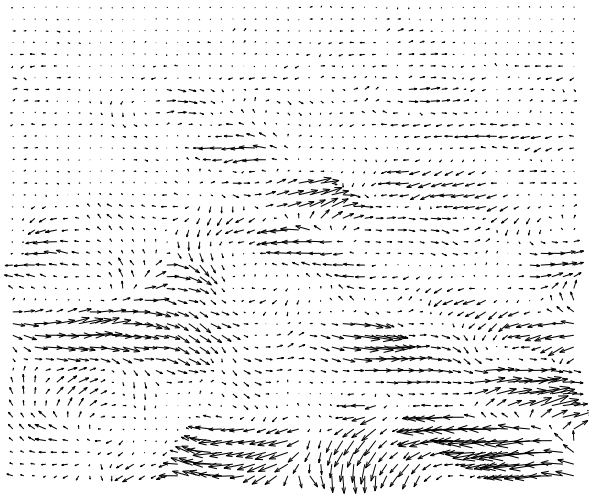

Figure 6: *First topos of the Bi-Orthogonal Decomposition of the alfalfa crop motion velocity field.*

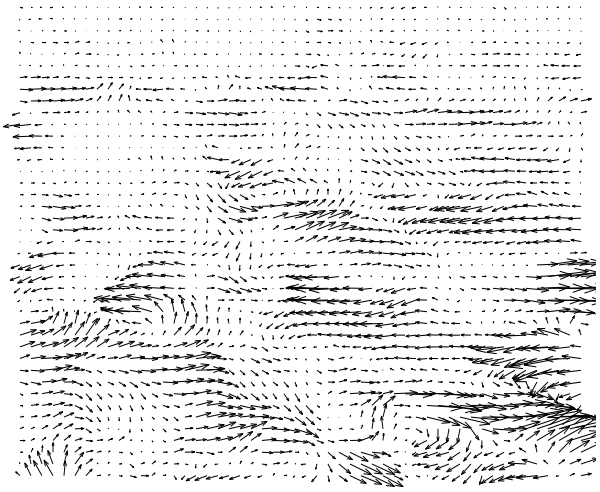

Figure 7: *Second topos of the Bi-Orthogonal Decomposition of the alfalfa crop motion velocity field.*

The next *topos* in the BOD series (not shown) are also composed of large coherent structures. Only the less energetic modes involved decorrelated motions.

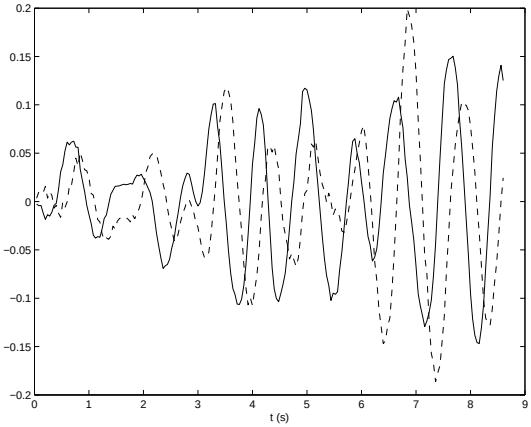

Figure 8: *First (—) and second chronos (- -) of the Bi-Orthogonal Decomposition of the alfalfa crop motion velocity field.*

The *chronos* (Figure 8) have a regular oscillating behavior with a common well defined frequency f of about 1.2 Hz, which is typical of alfalfa vibration (Doaré et al, 2004).

A more detailed analysis of the *topos* shows that there is a phase lag in space between the vorticity fields associated with *topos* 1 and 2. As the corresponding *chronos* are also phase lagged in time, the combination of these first two spatio-temporal modes would show propagative patterns. A phase velocity may be defined as $c = \Lambda f \approx 1.2$ m/s. Note that it is less than the mean wind velocity (4 m/s).

The next *chronos* in the decomposition also went by pairs and presented similar propagation properties with the same frequency as the most energetic *chronos*. It is remarkable that the BOD extracts a dominant temporal frequency, whereas it was impossible to detect one by eye.

Several movies of wheat and alfalfa crop motions under various wind conditions were analysed with this method. In all cases we found similar features as the ones presented here. The first modes of the BOD reveal the motion characteristics: large coherent propagative stuctures. The analysis of the *topos* and *chronos* allow to determine the spatial wavelength and the temporal frequency of the plants motion.

6. CONCLUSION

The present method associating video recording, PIV, and BOD analysis appears to be a promising technique to analyse wind induced motions in crops. It appears today as the only practical approach to get spatio-temporal information on the

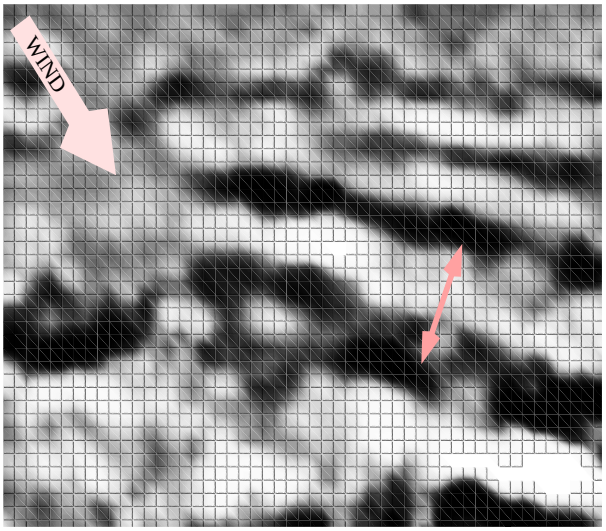

Figure 9: *Vorticity field of topos 1 (white stands for clockwise and black for counter-clockwise vorticity). The arrow represents a typical wavelength* Λ *of the coherent structures. The wind direction is approximative here.*

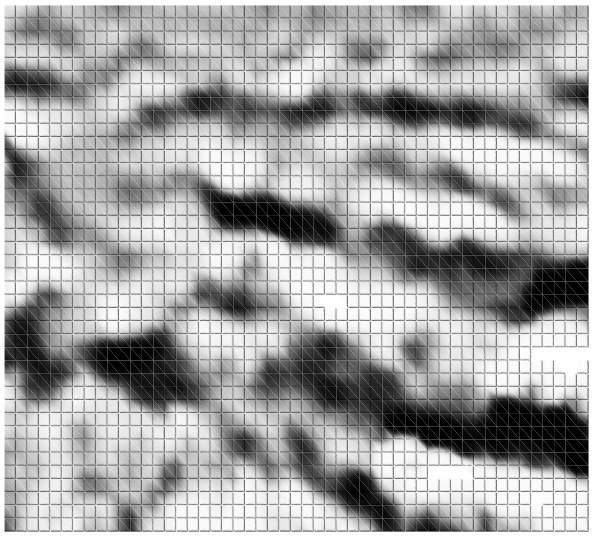

Figure 10: *Vorticity field of topos 2.*

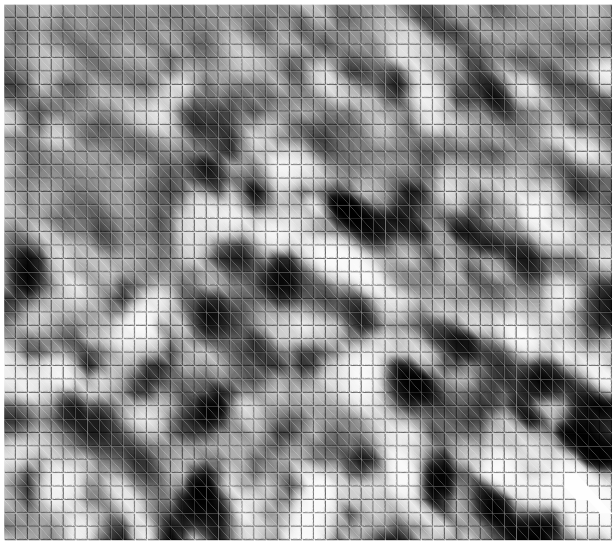

Figure 11: *Divergence field of topos 1 (white stands for positive divergence, and black for negative divergence).*

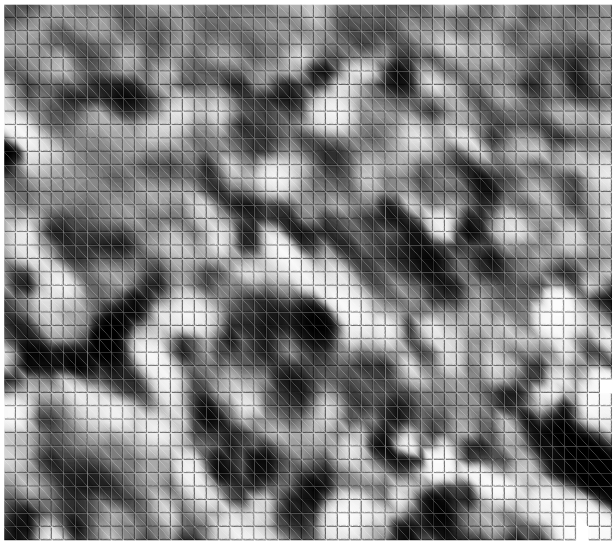

Figure 12: *Divergence field of topos 2.*

crops dynamics to compare with predictions of models on the coupling of the wind mixing layer over canopies and the plants motion (Doaré et al (2004), Py et al (2004)).

7. REFERENCES

Coutand C., Julien J.L., Moulia B., Mauget J.C., Guitard D., 2000, Biomechanical study of the effect of a controlled bending on tomato stem elongation. Global mechanical analysis, *Journal of Experimental Botany* **51**:1813-1824

Doaré O., Moulia B., de Langre E., 2004, Effect of plant interaction on wind-induced crop motion. Transactions of the ASME, *Journal of Biomechanical Engineering*, to appear **126**.

Farquhar T., Meyer H., van Beem J., 2000, Effect of aeroelasticity on the aerodynamics of wheat, *Materials Science and Engineering* **C7**:111-17

Flesch T.K., Grant R.H., 1992, Corn motion in the wind during senescence: I. Motion characteristics, *Agronomy Journal* **84**:742-747

Finnigan J., 2000, Turbulence in plant canopies. *Annual Review of Fluid Mechanics* **32**:519-571.

Hémon P., Santi F., 2003, Applications of biorthogonal decompositions in fluid-structure interactions, *Journal of Fluids and Structures* **17**:1123-1143

Py C., de Langre E., Moulia B., 2003, The mixing layer instability of wind over a flexible crop canopy, submitted to *C. R. Mecanique.*

Raffel M., Willert C.E., Kompenhans J., 1998, *Particle Image Velocimetry: a practical guide*, Springer-Verlag, Berlin, 3rd edition.

Raupach M.R., Finnigan J.J., Brunet Y., 1996, Coherent eddies and turbulence in vegetation canopies: the mixing layer analogy. *Boundary-Layer Meteorology*, **78**:351-382.